

# Compositional Imaging of Polystyrene and Low-Density Polyethylene Blend in Atomic Force Microscopy

Sergei Magonov, John Alexander, and Sergey Belikov  
SPM Labs LLC, 148 W. Orion Str. Tempe AZ 85283 USA

## Introduction

Comprehensive characterization of materials' surfaces is empowered with atomic force microscopy (AFM) - the technique that provides high-resolution visualization of surface structures and evaluation of their mechanical, electric and other properties. AFM studies are broadly applied for examination of polymer materials [1]. This is related to the fact that common AFM probes can induce a local deformation of these materials, whose elastic moduli varies in the range from few kPa to 10 GPa. The probe response in DC and AC AFM modes depends on local sample stiffness, and this is reflected in contrast of different AFM images. Therefore, visualization of polymer morphology and nanostructures is enhanced by recognition of samples' constituents with dissimilar mechanical properties. This capability provides compositional imaging of heterogeneous polymer materials such as block copolymers, polymer blends and composites. Typically, the constituents with various chemical nature exhibit different mechanical behavior. However, different packing of the same molecules can also lead to variations of mechanical properties of materials. In semicrystalline polymers (polyethylene, polypropylene and others) polymer chains either form crystalline lamellar structures by multiple chain folding or they are randomly oriented in amorphous material. This variation of local packing leads to difference of elastic moduli of crystalline and amorphous parts and their distinguishing in AFM images. A practical realization of compositional imaging of polymers is demonstrated below in our study of thin films prepared of atactic polystyrene (PS) and low density polyethylene (LDPE) blend on Si substrate. These polymers are characterized by elastic moduli, which is substantially larger in PS (3 GPa) than in LDPE (0.2-0.4 GPa). PS is amorphous polymer that is in glassy state at room temperature. LDPE is semicrystalline polymer, and it is composed of amorphous material, which is rubbery state at room temperature, and crystalline entity represented by lamellar structures. An overall crystallinity of LDPE is between 35% and 55% depending on sample preparation. PS-LDPE blend is often applied in AFM experiments, which demonstrate sensitivity of different modes (phase imaging, contact resonance, AFM-IR, etc) for a detection of the components and visualization of their distribution. However, not always the peculiarities of the blend composition and polymer structure are taking into account. A current report is intended to show how a detailed compositional study of PS-LDPE blend helps understanding a formation of polymer morphology and nanostructures in confined geometry of thin and ultrathin polymer films.

## Experimental

### *Samples and preparation*

For our study we prepared layers of polymer blend of atactic polystyrene (PS) and low density polyethylene (LDPE) on Si substrate. The pieces of FZ Si <100> wafer were used for the blend deposition. PS with molecular weight  $M_w = 106,000$  was purchased from Polymer Solutions Inc. LDPE was a gift from BP Chemicals. The polymers were dissolved in toluene, which was heated close to 100°C in case of LDPE to facilitate dissolution of this polymer. Few droplets of PS-LDPE solutions with concentrations of 5

mg/ml and 0.5 mg/ml were applied to the substrate in spin-casting procedure, which was performed at temperature around 100°C.

#### AFM measurements

AFM studies were performed in air with MultiMode microscope (Bruker), which was operated with NanoScope IIIA controller and new Phoenix controller (SPM Labs). The measurements were made in air using amplitude modulation (aka tapping [2]) mode with phase imaging (AM-PI). Si probes (Applied Nanostructures) with following nominal dimensions (*length,  $\mu\text{m}$ /width,  $\mu\text{m}$ /thickness,  $\mu\text{m}$ ): 125/35/4 125/35/2 and 225/30/1 were applied in the experiments. The probes' resonant frequency  $\omega_{\text{res}}$ , spring constant  $k$ , quality factor  $Q$  and inverse optical sensitivity ( $IOS$ ) were determined with Thermal Tune procedure, which is implemented with Dynamic Cantilever Calibrator [3] combined with NanoScope IIIa controller and imbedded into Phoenix controller. In most experiments we applied initial free amplitudes  $A_0$  in the range 3 – 60 nm and set-point amplitudes  $A_{sp} = 0.9-0.3 A_0$ . For phase imaging we used a convention that the phase signal, which is equals 0° at frequencies much lower than the probe resonance, gradual increases to become 90° at the resonance and approaches 180° at frequencies far above. The probe parameters and operating amplitudes were used for quantitative estimates of maximal forces and deformations in AM-PI mode and for an illustration of bifurcation phenomenon, which is common for this mode. The images with 512×512 format were collected in most experiments. Scanning rates of 0.5-0.8 Hz were used for areas from several to tens microns on side, and 1 Hz rate was applied for sub-micron imaging. The image treatment and analysis was performed with MountainsMap® software by Digital Surf (France).*

#### Results and Discussion

Surface morphology of PS-LDPE film, which was prepared with 5 mg/ml solution, is shown in height and phase images in **Fig. 1a-b**. Thickness of this film (~400 nm) was measured as a step between the top surface and substrate, which was opened by a scratch of the film with a sharp wooden stick.

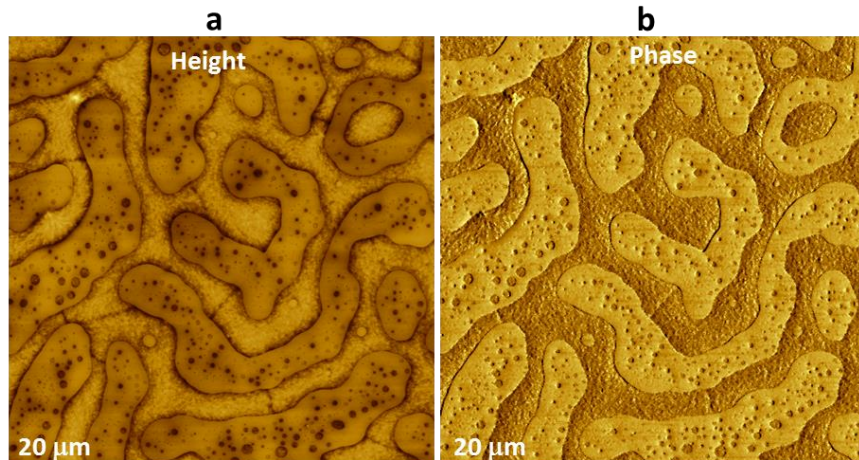


**Figure 1a-b.** Height and phase images of thin PS-LDPE film (thickness 400 nm) on Si substrate. In the study Si probe with  $k = 2.1 \text{ N/m}$  was used with amplitudes  $A_0 = 18 \text{ nm}$  and  $A_{sp} = 14 \text{ nm}$ .

The height image exhibits two types of surface regions with the micron-scale dimensions. The locations of one type are seen in height image as the slightly-darker curved ribbons with multiple circular depressions. The areas in between the ribbons with a fine structure and few smooth domains of a round shape can be allocated to another type. The assignment of these regions to the blend components is justified by their different phase contrast. The brighter ribbons represent one component, and another component occupies the circular depressions and the locations between the ribbons both exhibiting a darker phase contrast. Two surface regions, which are dominated by different components, are shown at higher magnification in **Figs. 2a-c** and **Figs. 3a-c**.

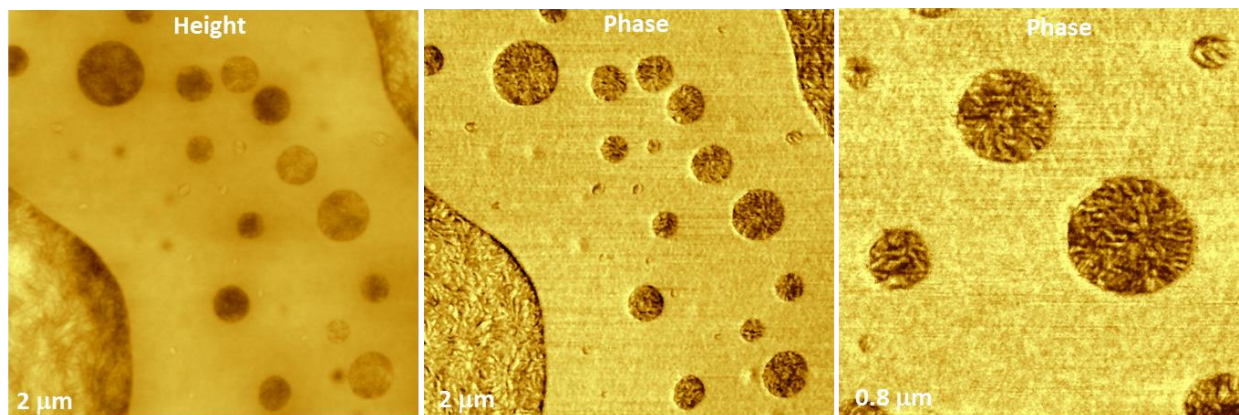


**Figure 2a-c.** Height and phase images of thin PS-LDPE film on Si substrate, which were recorded inside the area shown in **Figs. 1a-b**. In the study Si probe with  $k = 2.1$  N/m was used with amplitudes  $A_0 = 18$  nm and  $A_{sp} = 14$  nm.

A part of the ribbon in **Fig. 2a** exhibits a flat surface with depressions of different depth, which display a fine structure formed by short fibrils. Similar features are noticed outside the ribbon at the bottom left and top right corners of the image. The fibrils, most likely, represent surface regions with traces of lamellar structures of semicrystalline LDPE. The short fibrils are best resolved in the phase images (**Figs. 2b-c**), and their width matches the lamellar thickness of LDPE (10-20 nm) determined from X-ray diffraction and TEM data [4]. The assignment of the fine structure to polymer lamellae is consistent with overall phase contrast of these locations that is darker than that of the main part of the ribbon. Another surface location (**Fig. 3a-c**) is dominated by lamellar structures of LDPE, and only few round-shape domains, which are indicated with white arrows in **Fig. 3c**, can be assigned to PS. The height image of lamellar structure of this layer, which was obtained at low tip-force, is shown in **Fig. 4a**. It is characterized by nanostructures with a shape of the round or extended grains, which are emphasized in height image in **Fig. 4b**. The phase image of this location is quite different, **Fig. 4c**. Among dark phase features one can find few fibers (~20 nm in width) and several blocks of closely packed rods with spacings in the 10-15 nm range. These features can be assigned to the hard lamellar core, which is covered by an amorphous polymer that forms top surface of LDPE domain. This explanation is consistent with the earlier finding [5] and other data for different semicrystalline polymers [6].

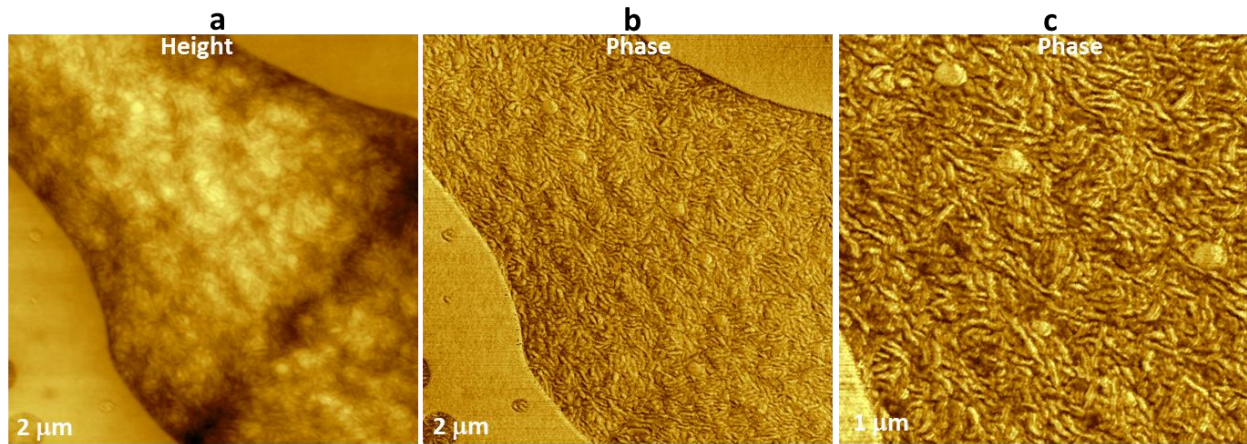


**Figure 3a-c.** Height and phase images of thin PS-LDPE film on Si substrate, which were recorded inside the area shown in **Figs. 1a-b**. In the study Si probe with  $k = 2.1$  N/m was used with amplitudes  $A_0 = 18$  nm and  $A_{sp} = 14$  nm.

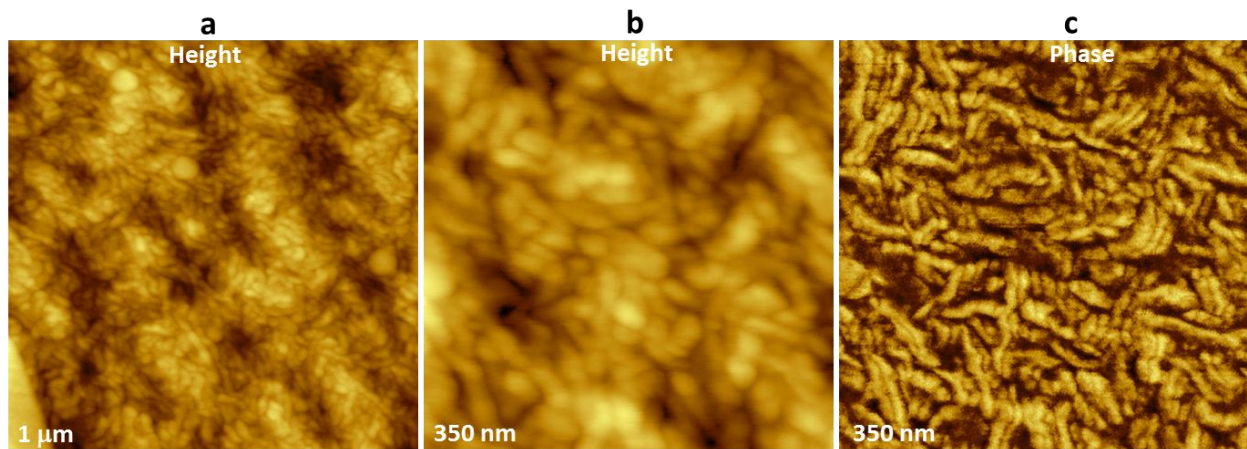


**Figure 4a-c.** Height and phase images of thin PS-LDPE film on Si substrate, which were recorded inside the area shown in **Figs. 3a-c**. In the study Si probe with  $k = 2.1$  N/m was used with amplitudes  $A_0 = 18$  nm and  $A_{sp} = 14$  nm.

It is worth noting that the images in **Figs. 1-4** were recorded with Si probe (125/35/2) with  $k = 2.1$  N/m, and their phase contrast has varied in the range of 5-7 degrees. The estimates of the maximal force and sample deformation, which is realized at the bottom of the oscillation cycle in AM-PI mode, were performed as described in [7] using Hertz model for the tip-sample interactions. These parameters depend not only on  $A_0$  and  $A_{sp}$  but also on elastic modulus of a sample location. The forces and deformations, which were realized in the images in **Figs. 1-3**, were around 1 nN and 0.2 nm for PS and 0.7 nN and 0.5 nm for LDPE. The images of the similar PS-LDPE film, which were obtained using another Si probe (125/35/4) with  $k = 24.4$  N/m, are shown in **Figs. 5a-b** and **Figs. 6a-b**. The images in **Fig. 5a-b** were obtained at  $A_0 = 4.8$  nm and  $A_{sp} = 4.3$  nm, and the images in **Fig. 6a-b** at  $A_0 = 11$  nm and  $A_{sp} = 4.3$  nm. The difference of the tip-sample interactions, which are  $\sim 1$  nN (PS), 0.7 nN (LDPE) and  $\sim 3$  nN (PS),  $\sim 2.2$  nN (LDPE) for images, respectively, in **Fig. 5** and **Fig. 6**, leads to a strong enhancement of the phase contrast from 5-6 degrees to over 100 degrees.

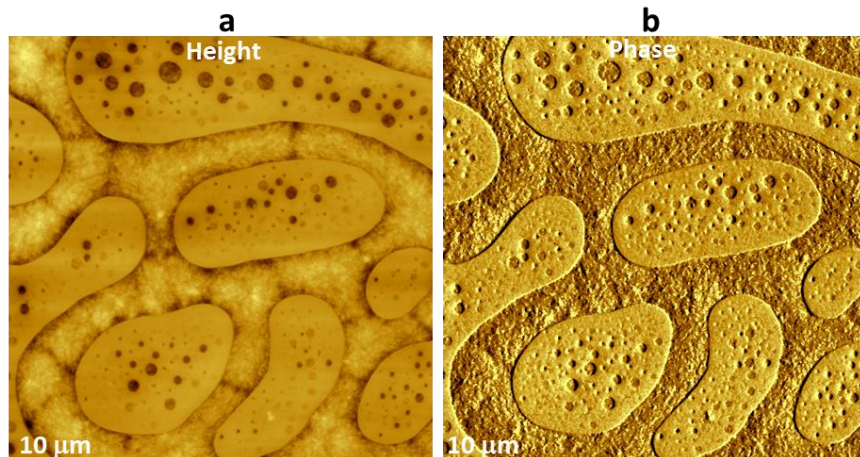


**Figure 5a-b.** Height and phase images of thin PS-LDPE film (thickness 400 nm) on Si substrate. In the study Si probe with  $k = 24.4$  N/m was used with amplitudes  $A_0 = 4.8$  nm and  $A_{sp} = 4.3$  nm.

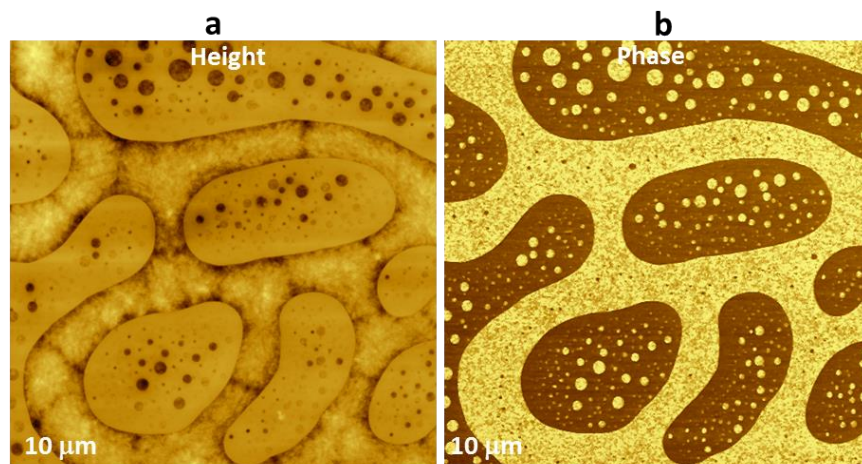


**Figure 6a-b.** Height and phase images of thin PS-LDPE film (thickness 400 nm) on Si substrate. In the study Si probe with  $k = 24.4$  N/m was used with amplitudes  $A_0 = 11$  nm and  $A_{sp} = 4.3$  nm.

This effect is analyzed in more details in the images shown in **Fig. 7a-e**, which present a region containing both blend components. A comparison of the phase images, which were recorded at different  $A_0$  and  $A_{sp}$  sets (**Fig. 7b-e**), shows that in the image with highest contrast (**Fig. 7c**) and partially in the image in **Fig. 7d** the lamellar features are not reproduced correctly. This is a consequence of bifurcation effect in AM-PI, which is related with instability of the probe at transition from attractive to repulsive force regime. This phenomenon is further explained in **Appendix**. In low force imaging (**Fig. 7b**) the phase contrast of lamellar structures reflects mostly the lamellar edges similar to that happened in amplitude (error signal) images of this mode. The lamellar contours became pronounced in phase image in **Fig. 7e**, which was recorded at  $A_0 = 16$  nm and  $A_{sp} = 4.3$  nm. At these conditions the probe is sensing the lamellar cores ( $\sim 15$  nm in width) that are seen distinctly inside circular LDPE sub-micron domains in **Fig. 7f**.

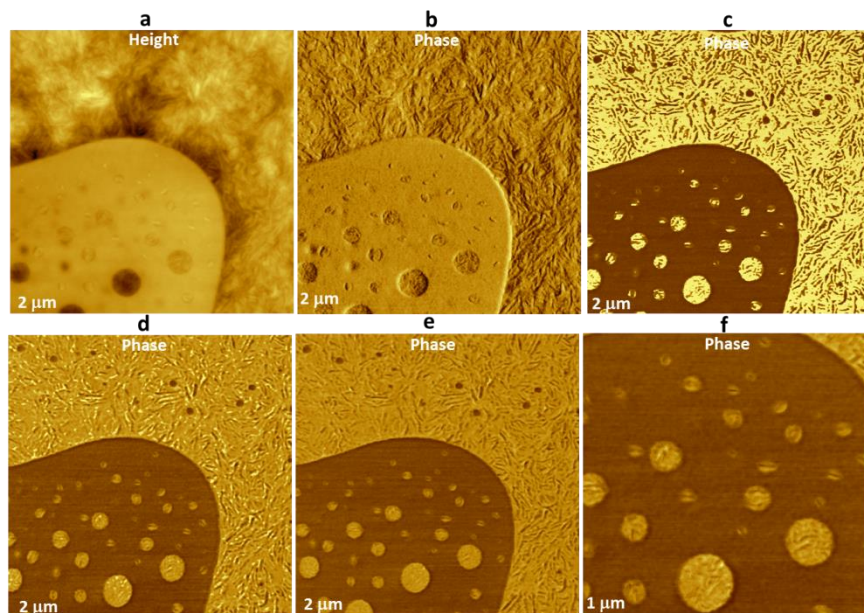


**Figure 7a-f.** Height and phase images of thin PS-LDPE film (thickness 400 nm) on Si substrate. In the study Si probe with  $k = 24.4$  N/m was used with amplitudes  $A_0 = 4.8$  nm and  $A_{sp} = 4.3$  nm (**a, b**);  $A_0 = 11$  nm and  $A_{sp} = 4.3$  nm (**c**);  $A_0 = 13$  nm and  $A_{sp} = 4.3$  nm (**d**); and  $A_0 = 16$  nm and  $A_{sp} = 4.3$  nm (**e, f**).

PS-LDPE film, which was prepared from 0.5 mg/ml solution, exhibits an overall binary morphology, in which slightly darker PS domains in height image in **Fig. 8a** are surrounded by the raised lamellar aggregates of LDPE. The darkest locations present the multiple voids of the film where the probe touches Si substrate. The height cross-section profiles, which are taken across the film and substrate regions, showed that the domains and aggregates are 10 nm - 15 nm thick.

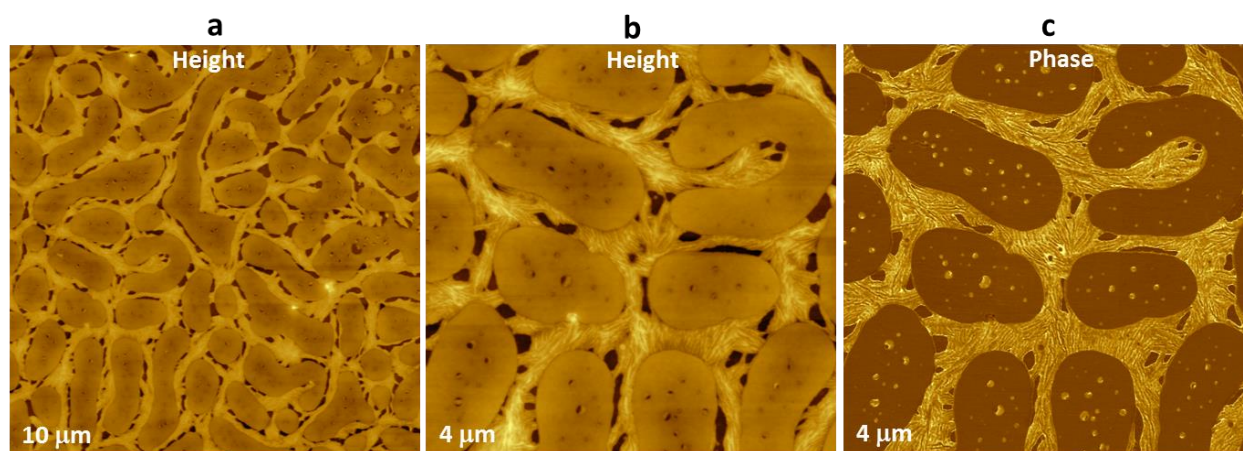


**Figure 8a-c.** Height and phase images of ultrathin PS-LDPE film (thickness  $\sim 15$  nm) on Si substrate. The images in (**b, c**) were recorded inside the area shown in (**a**). In the study Si probe with  $k = 2.1$  N/m was used with amplitudes  $A_0 = 12$  nm and  $A_{sp} = 10.6$  nm (**a**) and  $A_0 = 48$  nm and  $A_{sp} = 16$  nm (**b, c**).

The suggested assignment of the film regions is supported by height and phase images of a smaller area, which were obtained at high-force imaging, **Fig. 8b-c**. The extended linear structures of ~25 nm in width represent closely packed LDPE lamella, which are well resolved in height and phase images. These images allow proposing that in ultrathin film crystallization is more efficient than in the 400-nm thick film, and the formed lamellae became much longer. A close proximity of the substrate to the film material might be an important factor influencing LDPE crystallization. The lamellar architecture is most distinctive in the height and phase images in **Fig. 9a-c**. In height image in **Fig. 9a** one can observe grainy fringes of lamellar edges with some lamellae slightly leaning from their edge-on orientation. The lamellar tilt explains the variable separation between the neighboring linear features. In the phase images the lamellar structures are seen at low and high forces either due to the edge effects at low-force imaging (**Fig. 9b**) or due to strong material-related phase contrast at high-force imaging (**Fig. 9c**). The phase contrast in **Fig. 8c** and **Fig. 9c** allows distinguishing four surface components of this sample as it is shown in the phase profile in **Fig. 9d**. The darkest contrast relates to Si substrate that is 3-5 degree lower than the contrast of PS domains. The latter is 10-15 degrees below that of LDPE. The phase variations between the lamellar core and nearby amorphous polymer are in the range of 5-10 degrees. This example is a convincing illustration of AFM compositional imaging.

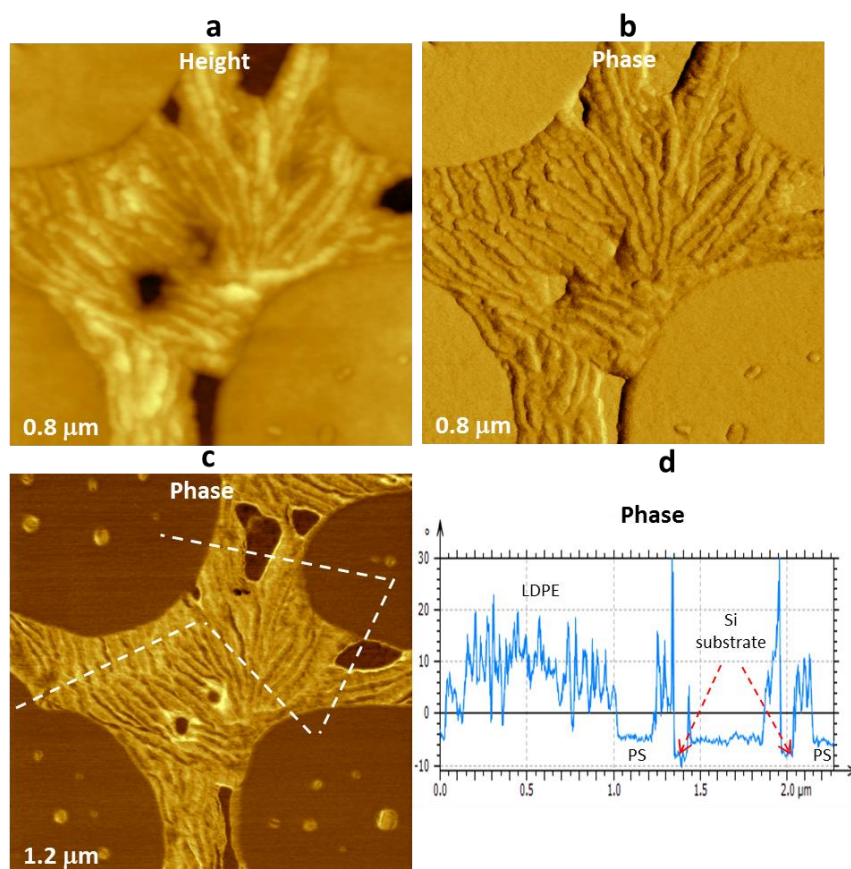


**Figure 9a-d.** (a-c) Height and phase images of ultrathin PS-LDPE film (thickness ~15 nm) on Si substrate. The images were recorded inside the area shown in **Fig. 8b**. In the study Si probe with  $k = 2.1$  N/m was used with amplitudes  $A_0 = 12$  nm and  $A_{sp} = 10.6$  nm (a, b) and  $A_0 = 48$  nm and  $A_{sp} = 16$  nm (c). (d) – The phase profile, which was taken in (c) along the trajectory shown with a dashed white line.

In sample preparation tests we have noticed another type of morphology (**Fig. 10a-c**) besides the above-discussed blend films that smoothly cover Si surface. A substantial dewetting of Si substrate by the blend during spin-casting might explain this surface organization. It is characterized by a large number of extended aggregates up to 50 nm in height and up to 1-2  $\mu\text{m}$  in width. The raised aggregates are spread over the sample surface, and they are surrounded by a thin layer with composite nanostructure. These features are best visible in the height and phase images in **Fig. 10b-c**. Nanoscale bands are resolved in the bottom layer, and they exhibit a brighter phase contrast compared to their surroundings, **Fig. 10c**.

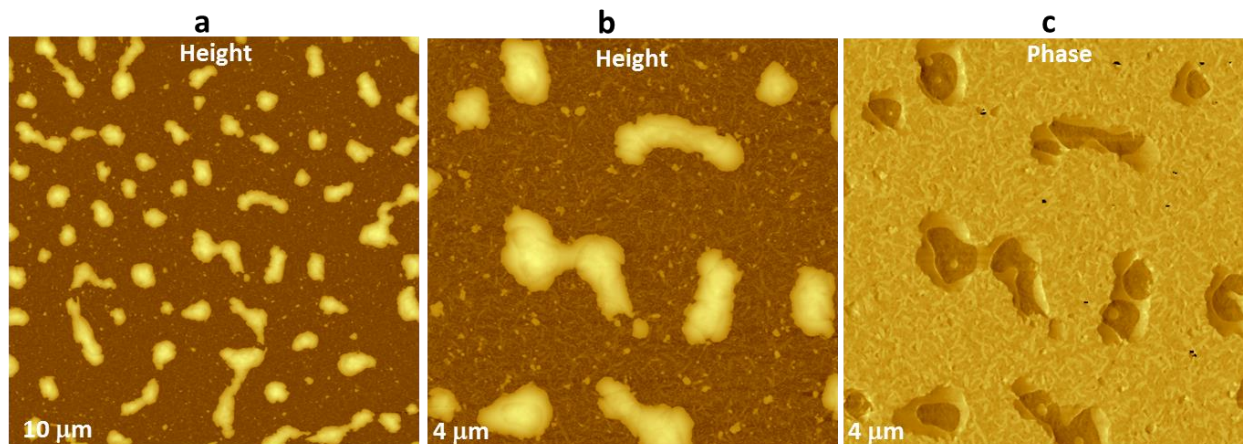


**Figure 10a-c.** Height and phase images of PS-LDPE film with complex morphology. The images in **(b, c)** were recorded inside the area shown in **(a)**. In the study Si probe with  $k = 0.69$  N/m was used with amplitudes  $A_0 = 12$  nm and  $A_{sp} = 10$  nm **(a)** and  $A_0 = 24$  nm and  $A_{sp} = 10$  nm **(b, c)**.

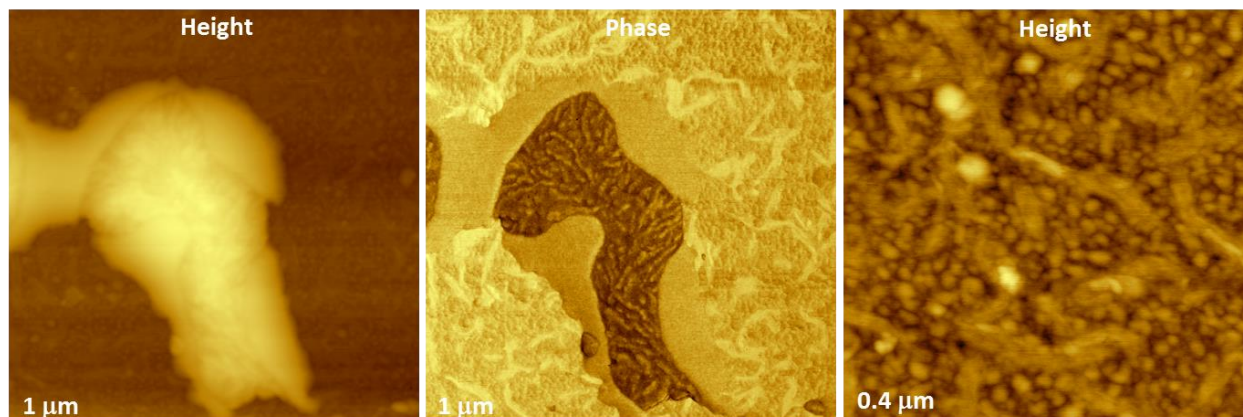


**Figure 11a-c.** Height and phase images of PS-LDPE film with complex morphology. The images were recorded inside the area shown in **Fig. 10b**. In the study Si probe with  $k = 0.69$  N/m was used with amplitudes  $A_0 = 24$  nm and  $A_{sp} = 10$  nm **(a, b)** and  $A_0 = 12$  nm and  $A_{sp} = 10$  nm **(c)**.

The aggregates have a complex structure, which is identified by faintly seen contours in the height image and more pronounced contrast variations in the phase image. The central part of the aggregates is darker than their edges and some inclusions. Therefore, they are composed of both polymers, and the higher magnification images (**Fig. 11a-b**) allow the assignment of the aggregates' parts. The central part

of one of the aggregates exhibits the lamellar structure that is well resolved in the phase images. The phase contrast of the outer part is featureless, and it is likely related to PS. Thus the aggregates are formed of central LDPE domains partially wrapped into PS material. The bottom layer is composed of band structures, which are surrounded by multiple grains of 10-20 nm in diameter. The height image in **Fig. 11c** shows that the bands are up to 200 nm in length and up to 30 nm in width. These features can be tentatively assigned to bundles of extended LDPE macromolecules, which are located among PS grains. The different phase contrast of these objects is in favor of this suggestion.

## Conclusions

Compositional imaging in AFM using oscillatory AM-PI mode is illustrated on films prepared from polymer blend of PS and LDPE on Si substrate. Recognition of surface regions enriched in PS and LDPE was based on visualization of specific structural features such as lamella of semi-crystalline LDPE and sensitivity of phase contrast to mechanically dissimilar locations. The latter helps to identify the surface areas occupied by the substrate, PS and amorphous and lamellar components of LDPE. Furthermore, AFM probe can depress a top surface amorphous layer of LDPE, which is substantially softer than the lamellar structures, and feel an underlying lamellae core. The demonstrated compositional imaging has revealed different types of micro-phase separation in PS-LDPE films and the lamellar organizations in thin and ultrathin layers. The observed structural variations are caused by specifics of polymer crystallization in different confined geometries. The optimization of AFM mapping of heterogeneous materials using the probes with different stiffness and by operating at various initial and set-point amplitudes was discussed. A particular phenomenon of bifurcation that complicates the image analysis and interpretation is considered in **Appendix**.

## References

- [1] S. Magonov "AFM in Analysis of Polymers" Encyclopedia of Analytical Chemistry, (R. A. Meyers, Ed.), pp. 7432-7491, John Wiley & Sons Ltd, Chichester, **2000**.
- [2] Q. Zhong, D. Innis, K. Kjoller, and V. Elings "Fractured polymer/silica fiber surface studied by tapping mode atomic force microscopy" *Surf. Sci. Lett.* **1993**, *290*, L688–L692.
- [3] J. Alexander, S. Belikov, S. Magonov, and M. Smith "Evaluation of AFM probes and instruments with dynamic cantilever calibrator" *MRS Advances* **2018**, 1-7 doi: 10.557/adv.2018.102
- [4] J. Lu, and H.-J. Sue "Morphology and mechanical properties of blown films of a low-density polyethylene/linear low-density polyethylene blend" *J. Polym. Sci. B: Polym. Phys.* **2002**, *40*, 507–518.
- [5] S. Magonov, and Yu. Godovsky "Atomic Force Microscopy, part 8. Visualization of sub-lamellar structure in crystalline polymers" *Amer. Lab.* **1999**, *31*, 52-58.
- [6] T. Hugel, G. Strobl, and R. Thomann "Building lamellae from blocks: The pathway followed in the formation of crystallites of syndiotactic polypropylene" *Acta Polym.* **1999**, *50*, 214-217.
- [7] S. Belikov, J. Alexander, C. Wall, and S. Magonov "Tip-sample forces in atomic force microscopy: Interplay between theory and experiment" *Mater. Res. Soc. Symp. Proc.* **2013**, Vol. 1527, DOI: 10.1557/opl.2013.

## Appendix

The probe-sample force interactions and dynamics of the oscillating cantilever play a crucial role in AM-PI mode but they can complicate the analysis of height and phase images recorded on heterogeneous samples. The behavior of similar non-linear oscillations has been thoroughly described in classical literature [A1]. A consideration of non-linear effects in AM-PI mode has been confined to analysis of the probe frequency and phase responses when the driving frequency has varied near the probe resonance and to a consideration of amplitude-versus-distance (AvZ) and phase-versus-distance (PvZ) dependencies at the probe resonance [A2]. A schematic description of these dependencies is given in **Fig. A1**.

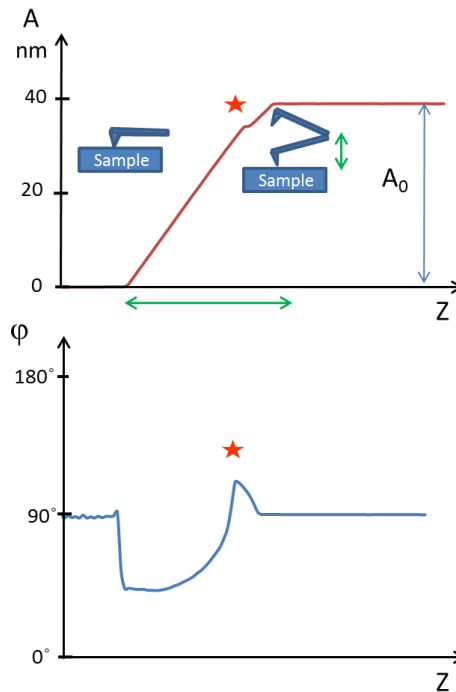


**Figure A1.** The amplitude-versus-distance (top) and phase-versus-distance (bottom) dependencies, which were measured on Si substrate using Si probe with spring constant  $k = 26.5$  N/m. The initial free amplitude  $A_0 = 40$  nm. The green lines show the tip-sample separation that is equals to  $A_0$ . In the illustration with AFM probe this distance is artificially reduced.

As the oscillating probe comes into periodical interactions with a sample the probe amplitude gradually drops and a change of its slope can be observed. At the point, which is marked with a red star, phase abruptly crosses  $90^\circ$  level. Initially, the phase has increased in response to tip-sample attractive interactions, and at this separation it has decreased sharply due to raised repulsive interactions. Depending on magnitude of  $A_0$ , sample material, tip apex dimensions and probe stiffness such phase transitions can extremely sharp and can happen at different  $A_{sp}$ . This phenomenon - saddle-node bifurcation has been observed in simulated and experimental AvZ and PvZ curves [A3]. A simulation of probe-sample force interactions in AM-PI mode in terms of asymptotic Krylov-Bogolujbov-Mitropolsky approach [A3-A4] has revealed that the abrupt changes in phase curves and the kinks on the amplitude curves are consistent with the transitions between two branches representing stable steady-state

solutions of asymptotic amplitude-phase dynamics. In practice, the system can accommodate one of the branches and jump to another one due to any small perturbation of tip-sample force interactions. This effect can influence the height and phase images as it was observed in the paper (**Fig. 7a-f**) and is shown below.

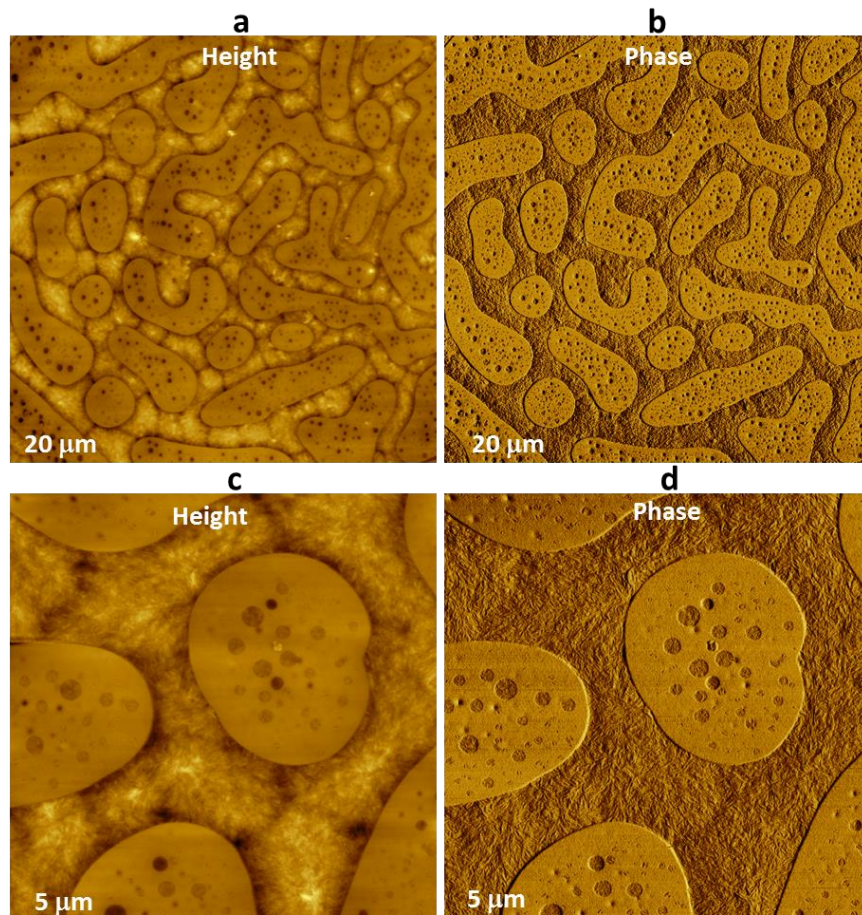


**Figure A2a-d.** Height and phase images of PS-LDPE thin film on Si substrate at two different scales. The images were obtained using Si probe with  $k = 7.3$  N/m and  $A_0 = 6$  nm and  $A_{sp} = 5$  nm.

The example, which illustrates the bifurcation effect in the height and phase images of PS-LDPE, is taken from study of thin film of the blend using Si probe with  $k = 7.3$  N/m. The height and phase images of this sample at two different areas shows the common morphology of the film, **Fig. A2a-d**. The bright phase contrast is observed on PS domains, which are slightly lower in height than the nearby lamellar structures of LDPE. Smaller inclusions of other component are noticed in PS domains and LDPE regions. Small PS particles are better seen in the images of sub-micron lamellar regions as that presented in **Fig. A3a-d**. The height and phase images of this location, which were recorded at four sets of  $A_0$  and  $A_{sp}$  amplitudes, exhibit pronounced changes. The observed image variations can be explained by bifurcation effect that happened on PS and LDPE structures. At low tip-sample forces, when the  $A_0$  is relatively small (14 nm) and  $A_{sp} = 12$  nm is close to  $A_0$ , the height image represents the topmost grains and short rods of this LDPE location, **Fig. A3a**. The related phase images exhibit minor changes according to the cross-

section profile on the right side of the image. These small phase variations reproduce surface corrugations similar to the amplitude (error) images of AM-PI mode.

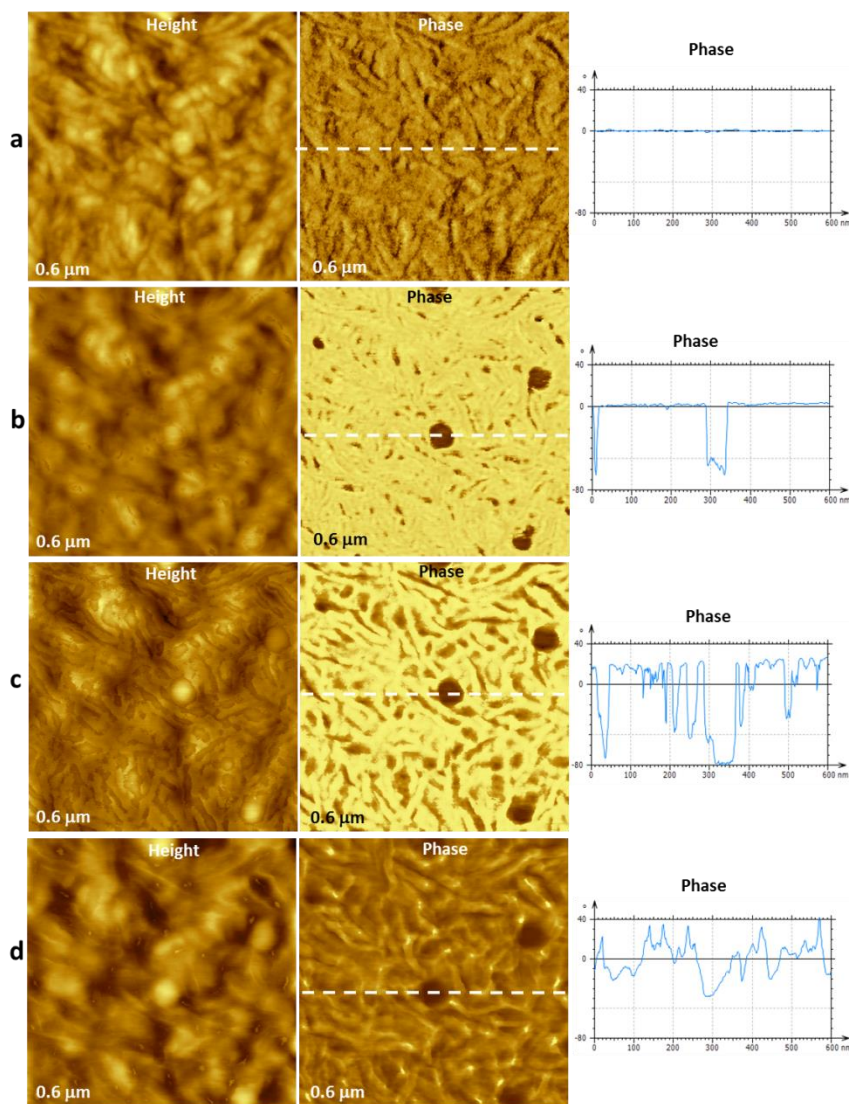


**Figure A3a-d.** Height and phase images with the cross-section phase profiles, which were taken along the direction indicated in the images with a white dashed line. The images were recorded using Si probe with  $k = 7.3 \text{ N/m}$ . The images were obtained with  $A_0 = 14 \text{ nm}$ ,  $A_{sp} = 12 \text{ nm}$  (a); with  $A_0 = 24 \text{ nm}$ ,  $A_{sp} = 12 \text{ nm}$  (b),  $A_0 = 36 \text{ nm}$ ,  $A_{sp} = 12 \text{ nm}$  (c); and  $A_0 = 64 \text{ nm}$ ,  $A_{sp} = 12 \text{ nm}$  (d).

As the initial amplitude was increased to 24 nm and  $A_{sp}$  remains the same, the images have changed with most variations noticed in the phase pattern, **Fig. A3b**. Numerous dark spots on the raised locations have perturbed the height image. The phase contrast has drastically increased from few degrees to  $\sim 60$  degrees on a number of surface features including those that were disturbed in the height image. They might represent the edges of most protruded lamellar structures. Four round-shaped domains with dark phase contrast can be assigned to PS inclusions. This suggestion is further supported by the images in **Fig. A3c**, which were recorded at higher  $A_0$  (36 nm) and  $A_{sp} = 12 \text{ nm}$ . In these images the perturbations

of height contrast occupied a half of the area, the round-shaped domains have risen over the surface, and the dark phase contrast became seen on most edge-on lamellar structures. These observations can be explained by the fact that with the increase of  $A_0$  transition from repulsive force regime, which has started at few PS domains and some lamella, has intensified on other lamellar structures and brought artifacts to the height image. The bifurcation effects on PS, LDPE lamellae and amorphous material are likely proceed at different amplitude conditions, and this can explain the observed complexity to the height and phase contrast. At these conditions the phase variations are substantially magnified to above 100 degrees as seen in the cross-section profile. Therefore, this is the best condition for compositional imaging of PS-LDPE blend but one should be aware about the related artifacts in the height image. Further increase of  $A_0$  to 60 nm led to the height and phase images shown in **Fig. 3Ad**. The structures observed in height image are quite different from those in the low-force height image in **Fig. 3Aa**. The pronounced PS domains and thin edges of the lamellae can be explained by stronger deformation of soft amorphous LDPE material. This is followed by a transformation of top surface profile in the height image to map of local stiffness. The estimates of maximal deformation of PS and LDPE locations for this  $A_0$  gives  $\sim 2$ nm that is close to the difference between their heights in **Fig. A3d**. The phase images in **Fig. A3d** closely resembles the features of the corresponding height image, and the phase variations become moderate as seen from the related cross-section profile. These observations are likely a consequence of the operation in strong repulsive regime. This example of AFM study of PS-LDPE film at different  $A_0$  and  $A_{sp}$  will be helpful for researchers dealing with compositional imaging of soft heterogeneous samples.

## References

- [A1] N. Bogoliubov, and Yu. Mitropolsky, "Asymptotic Methods in the Theory of Nonlinear Oscillations", Gordon & Breach, NY, **1961**.
- [A2] A. Kuehle, A. H. Sorensen, and J. Bohr, "Role of attractive forces in tapping tip force microscopy" *J. Appl. Phys.* **1997**, *81*, 6562–6569.
- [A3] S. Belikov, N. Yerina N. A. and S. Magonov, "Interplay between an experiment and theory in probing mechanical properties and phase imaging of heterogeneous polymer materials" *J. Physics, Conference Series*, **2007**, *61*, 765-769.
- [A4] S. Belikov, and S. Magonov, "Classification of dynamic Atomic Force Microscopy control modes based on asymptotic nonlinear mechanics" *Proceed. Amer. Control Conf.*, St. Louis, **2009**, 979-985.